Acta Radiol OnlineFirst, published on October 24, 2014 as doi:10.1177/0284185114554823

Review Article

Acta Radiologica
0(0) 1–9

DOI: 10.1177/0284185114554823
acr.sagepub.com
SAGE

Correlation between whole tumor size and solid component size on high-resolution computed tomography in the prediction of the degree of pathologic malignancy and the prognostic outcome in primary lung adenocarcinoma

Hisashi Saji[1,4], Jun Matsubayashi[2], Soichi Akata[3], Yoshihisa Shimada[1], Yasufumi Kato[1], Yujin Kudo[1], Toshitaka Nagao[2], Jinho Park[3], Masatoshi Kakihana[1], Naohiro Kajiwara[1], Tatsuo Ohira[1] and Norihiko Ikeda[1]

Abstract

Background: The presence of ground glass opacity (GGO) on high-resolution computed tomography (HRCT) is well known to be pathologically closely associated with adenocarcinoma in situ.

Purpose: To determine whether it is more useful to evaluate the whole tumor size or only the solid component size to predict the pathologic high-grade malignancy and the prognostic outcome in lung adenocarcinoma.

Material and Methods: Using HRCT data of 232 patients with adenocarcinoma who underwent curative resection, we retrospectively measured the whole tumor and solid component sizes with lung window setting (WTLW and SCLW) and whole tumor sizes with a mediastinal window setting (WTMW).

Results: There was significant correlation between the WTLW and the measurements of pathological whole tumor (pWT) ($r=0.792$, $P<0.0001$). The SCLW and WTLW values significantly correlated with the area of pathological invasive component (pIVS) ($r=0.762$, $P<0.0001$ and $r=0.771$, $P<0.0001$, respectively). The receiver operating characteristics area under the curve for WTLW, SCLW, and WTMW used to identify lymph node metastasis or lymphatic or vascular invasion were 0.693, 0.817, and 0.824, respectively. Kaplan-Meier curves of disease-free survival (DFS) and overall survival (OS) were better divided according to SCLW and WTMW, compared with WTLW. Multivariate analysis of DFS and OS revealed that WTMW was an independent prognostic factor (HR = 0.72, 95% confidence interval [CI] = 0.58–0.90, $P=0.004$ and HR = 0.74, 95% CI = 0.57–0.96, $P=0.022$, respectively).

Conclusion: The predictive values of the solid tumor size visualized on HRCT especially in the mediastinal window for pathologic high-grade malignancy and prognosis in lung adenocarcinoma were greater than those of whole tumor size.

Keywords
Lung adenocarcinoma, prognosis, solid component, ground glass nodule, high-resolution computed tomography

Date received: 19 May 2014; accepted: 17 September 2014

Introduction

The National Lung Screening Trial demonstrated a significant reduction in mortality from lung cancer with low-dose CT screening of 20.0% (95% confidence interval [CI], 6.8–26.7; $P=0.004$) (1). Recent advances in

[1]Department of Thoracic Surgery, Tokyo Medical University, Tokyo, Japan
[2]Department of Anatomic Pathology, Tokyo Medical University, Tokyo, Japan
[3]Department of Radiology, Tokyo Medical University, Tokyo, Japan
[4]Department of Chest Surgery, St. Marianna University School of Medicine, Kanagawa, Japan

Corresponding author:
Hisashi Saji, MD, PhD Associate Professor Department of Chest Surgery, St. Marianna University School of Medicine 2-16-1 Sugao, Miyamae-ku, Kawasaki, Kanagawa 216-8511, Japan.
Email: saji-q@ya2.so-net.ne.jp

high-resolution computed tomography (HRCT) and the widespread application of CT screening due to the positive results of screening CT trial have enhanced the discovery of small lung cancers, particularly adenocarcinoma (1). These often contain a non-solid component that presents as ground glass opacity (GGO) features on HRCT. Several investigators have reported that GGO is closely associated with bronchioloalveolar carcinoma (BAC) (2).

Recently, the International Association for the Study of Lung Cancer, the American Thoracic Society, and the European Respiratory Society proposed a new classification of lung adenocarcinoma. The terms BAC and mixed subtype adenocarcinoma are no longer used. For resected specimens, new concepts have been introduced such as adenocarcinoma in situ (AIS) and minimally invasive adenocarcinoma (MIA) for small solitary adenocarcinomas with either pure lepidic growth: AIS or predominantly lepidic growth with 5 mm invasion and MIA to define patients who, if they undergo complete resection, will have 100% or near 100% disease-specific survival rates, respectively (3,4). We therefore hypothesized that the GGO component is not related to malignancy or prognosis, implying that only the solid component of the tumor on HRCT (solid tumor size) is indicative of malignancy and prognosis in lung adenocarcinoma.

In this study, we first compared the whole tumor and solid component size, excluding areas of GGO, on preoperative HRCT with a lung window setting and whole tumor size with a mediastinal window setting with pathological whole tumor size and the area of pathologically confirmed invasion. We then determined whether it is more useful to evaluate the whole tumor size or that of only the solid component size to predict the degree of malignancy including lymph node involvement, lymphatic invasion, or vascular invasion of tumors in lung adenocarcinoma.

Material and Methods

Patients

Using preoperative HRCT data of 277 consecutive patients with adenocarcinoma who underwent curative surgical resection from January 2005 to December 2007, we retrospectively measured the whole tumor size and solid component size as follows: the whole tumor and solid component size was measured with lung window setting (WTLW and SCLW) and whole tumor size, with a mediastinal window setting (WTMW) on HRCT. Staging was determined according to the 7th edition of the TNM staging system (5). The histological tumor type was determined according to the World Health Organization (WHO) classification, 3rd edition. In addition, we measured the maximum size of the area pathologically confirmed invasion for this study. We excluded 21 patients with adenocarcinoma with scattered invasive components for this analysis, due to difficulty in measuring not only the pathological invasive area but also the size of the solid component radiologically. Twenty-four patients with inappropriate tissue samples were also excluded following induction therapy or divided tumor resection due to intraoperative frozen diagnosis. Ultimately, 232 consecutive patients with adenocarcinomas were enrolled in this study. Radiological and pathological findings were conducted by SA and JP, and JM and TN, respectively, who were blinded from any clinical information.

Patients were examined at 3-month intervals for the first 2 years and at 6-month intervals for the next 3 years and thereafter on an outpatient basis. The follow-up evaluation involved the following procedures: physical examination, chest radiography, CT of the chest and abdomen, and blood examination, including that of pertinent tumor markers. Further evaluations, including brain magnetic resonance imaging or CT, bone scintigraphy and integrated positron emission tomography, were performed on the first appearance of any symptom or sign of recurrence. The median follow-up time of this series was 4.4 years.

HRCT scanning

Chest images were obtained using 64-detector row CT scanners (LightSpeed VCT: GE Healthcare, Milwaukee, WI, USA and SOMATOM Sensation Cardiac 64: Siemens Medical Systems, Erlangen, Germany) and a 16-detector row CT scanner (BrightSpeed Elite: GE Healthcare, Milwaukee, WI, USA). High-resolution images of the tumors were acquired using the following parameters: 120 kV and auto exposure control; collimation, 0.6–1.25 mm; pitch, 0.9–0.984; 0.4–0.5 s per rotation; reconstructed interval, 1.25–1.5 mm; pixel resolution, 512 × 512; field of view, 20 cm; and a lung window settings (level = −500/width = 1500 HU) with high spatial frequency algorithm and mediastinal window settings (level = 40/width = 320 HU) with soft-tissue algorithm. GGO was defined as an increase in lung attenuation that did not obscure the underlying vascular markings. We defined the solid tumor size as the maximum dimension of the solid component of the lung windows excluding GGO (SCLW) or the maximum dimension of the whole tumor size of mediastinal setting (WTMW) (Fig. 1a and b).

Pathological findings

Histopathological studies were performed according to WHO criteria, 3rd edition (6). All resected

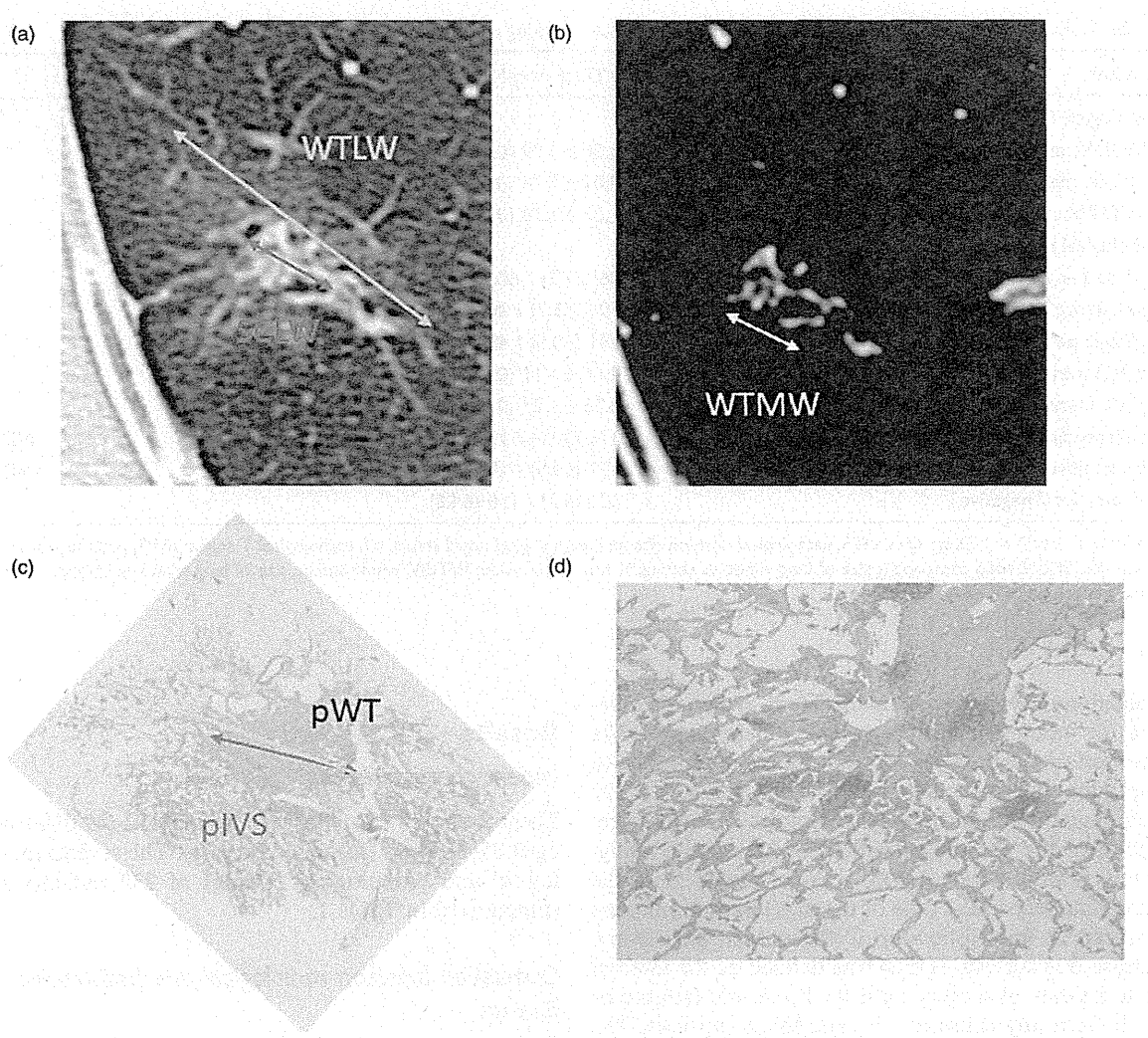

Fig. 1. Correlation between radiological and pathological findings in one typical case. WTLW and SCLW (a), WTMW (b), pWT and pIVS (c), pathological invasive area with high magnification (d). pIVS, pathologically confirmed invasion size; pWT, pathologically confirmed whole tumor size; SCLW, solid component size of lung windows setting; WTLW, whole tumor size of lung windows setting; WTMW, whole tumor size of mediastinal setting.

specimens were formalin-fixed and stained with hematoxylin and eosin in the routine manner. For detailed examinations of lymphatic or vascular invasion or pleural invasion, Elastica van Gieson stain was used to evaluate histological structure and tumor invasion. We also assessed several histological factors: (i) pathological nodal status (pN); (ii) vascular (v) or lymphatic (ly) invasion; and (iii) degree of tumor differentiation (well [G1], moderate [G2], poor [G3]). The maximum size of the pathological whole tumor (pWT) and of the pathological invasive component were measured (pIVS). The maximum size of pWT was assessed by standard gross measurement or histological reconstruction, as necessary. The maximum size of the invasive component was measured microscopically. If the tumor was large, the maximum size of the invasive area was calculated by reconstruction of the tumor slides and measured (Fig. 1c and d). Pathologic high-grade malignancy was defined as lymph node involvement, lymphatic invasion, or vascular invasion.

Statistical analysis

The data are presented as numbers and percentages or mean ± standard deviation, unless otherwise stated. The receiver operating characteristic curves of the whole and solid tumor sizes were used for the

Table 1. Radiological and pathological findings of 232 patients with lung adenocarcinoma.

Variables	*n* (% or range)	
Radiological findings		
WTLW: mean ± SD (cm)	2.59 ± 1.09 (0.73–6.84)	
SCLW: mean ± SD (cm)	2.01 ± 1.18 (0.00–5.78)	
WTMW: mean ± SD (cm)	1.87 ± 1.18 (0.00–5.71)	
Pathological findings		
pT status: pT1a / pT1b / pT2a / pT2b / pT3	86 (37.2) / 68 (29.2) / 61 (26.2) / 6 (2.7) / 11 (4.7)	
pN status: pN0 / pN1 / pN2	195 (83.7) / 20 (8.6) / 17 (7.7)	
pStage: pIA / pIB / pIIA / pIIB / pIIIA	141 (60.5) / 48 (20.6) / 8(3.4) / 8 (3.4) / 27 (12.1)	
pWT: mean ± SD, cm	2.61 ± 1.11 (0.90–7.20)	
pIVS: mean ± SD, cm	2.26 ± 1.27 (0.00–7.2)	
Differentiated: well or poorly	118 (50.6) / 107 (45.9)	ND: 8
Ly: positive / negative	127 (54.5) / 102 (43.8)	ND: 3
V: positive / negative	82 (35.2) / 150 (64.8)	

Ly, lymphatic invasion; ND, no data; pIVS, pathological invasion size; pN, pathological nodal status; pT, pathological T status; pWT, pathological whole tumor size; SCLW, solid component size of lung windows setting; V, vascular invasion; WTLW, whole tumor size of lung windows setting; WTMW, whole tumor size of mediastinal setting.

prediction of lymph node involvement, lymphatic invasion, or vascular invasion or well differentiation. We also performed multiple logistic regression analysis to determine the independent variables related to the whole tumor size and the solid tumor size for the prediction of the pathologic finding of high-grade malignancy. Overall survival (OS) was calculated from the date of surgery to the time of death. Observations were censored at final follow-up if the patient was living. Disease-free survival (DFS) was defined as the interval from the date of surgery until the first event (relapse or death from any cause) or the last follow-up visit. The duration of DFS was analyzed using the Kaplan-Meier method. Differences in OS or DFS were assessed using the log-rank test. To assess the potential independent and valuable prognostic effects of clinical tumor size on OS or DFS, we performed multivariate analysis with the Cox proportional hazards model using variables with $P < 0.05$. The data were statistically analyzed using the Statistical Package for Social Sciences software, version 10.5 (SPSS Inc., Chicago, IL, USA).

Ethical considerations

The approval of the Institutional Review Board of Tokyo Medical University was obtained (project approval No. 1665), but as this was a retrospective study the need to obtain written informed consent from either the patients or their representatives was waived, in accordance with the American Medical Association Manual of Style (10th edition).

Results

Patient characteristics

There were 118 (51.0%) women and 114 (49.0%) men aged 35–86 years (mean, 65.0 years). The several radiological and pathological findings of 232 patients are summarized in Table 1.

Correlation between radiological and pathological findings

Fig. 2 shows several correlations between radiological findings including WTLW, SCLW, or WTMW, and pathological findings including pWT or pIVS. There were significant correlations between SCLW and pIVS ($R = 0.762$, 95% CI = 0.702–0.811, $P < 0.0001$), WTMW and pIVS ($R = 0.771$, 95% CI = 0.713–0.819, $P < 0.0001$), and WTLW and pIVS ($R = 0.792$, 95% CI = 0.735–0.835, $P < 0.0001$), respectively.

Receiver operating characteristic curve

The receiver operating characteristic area under the curve values of WTLW, SCLW, WTMW, and pIVS used for predicting lymph node involvement, lymphatic invasion, vascular invasion, degree of differentiation, and pathologic high-grade malignancy (lymph node involvement or lymphatic or vascular invasion) are given in Table 2 and Fig. 3. The predictability of all outcomes on the basis of solid tumor size such as SCLW and WTMW was better than that using the

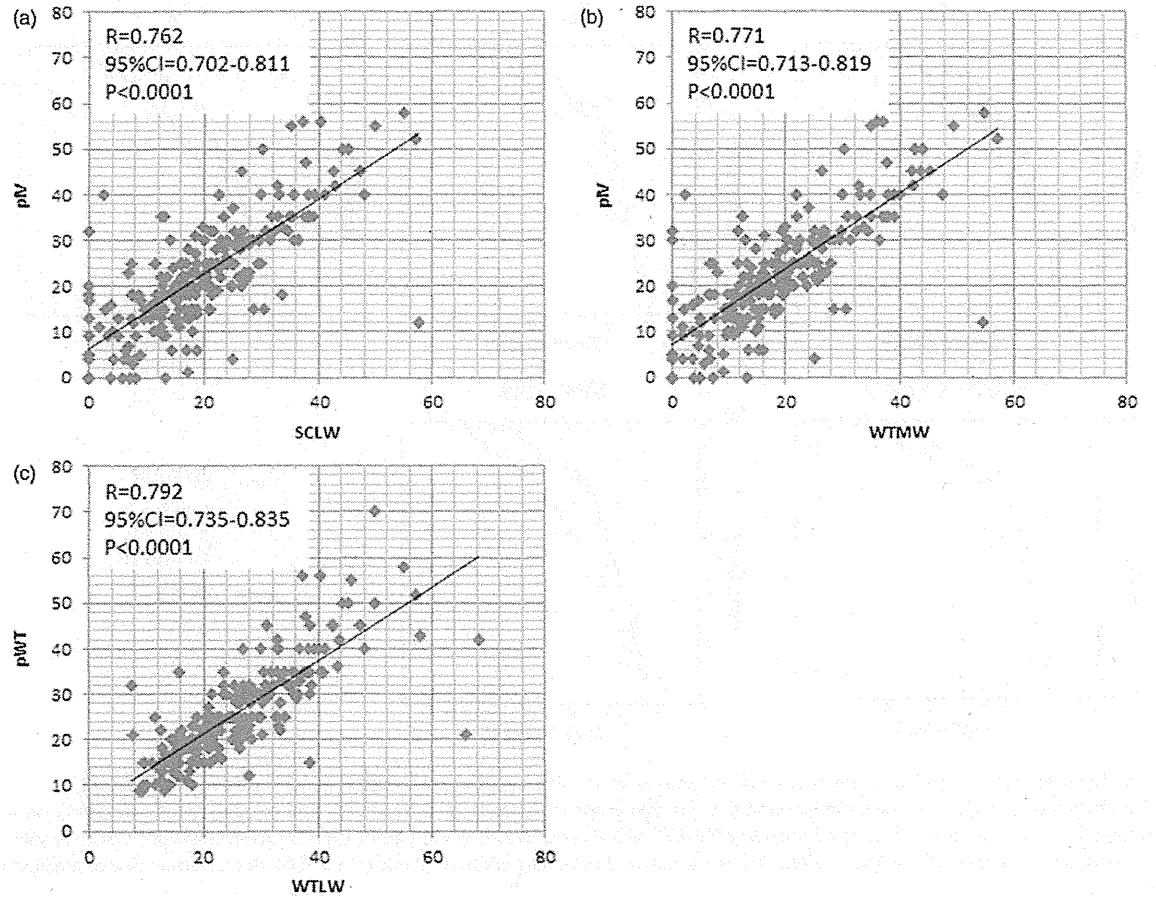

Fig. 2. Correlative graphs between radiological and pathological findings. There were significant correlations between SCLW and pIVS (R = 0.762, 95% CI = 0.702–0.811, $P < 0.0001$) (a), WTMW and pIVS (R = 0.771, 95% CI = 0.713–0.819, $P < 0.0001$) (b), and WTLW and pIVS (R = 0.792, 95% CI = 0.735–0.835, $P < 0.0001$) (c), respectively. pIVS, pathologically confirmed invasion size; pWT, pathologically confirmed whole tumor size; SCLW, solid component size of lung windows setting; WTLW, whole tumor size of lung windows setting; WTMW, whole tumor size of mediastinal setting.

Table 2. Receiver operative characteristic area under the curve values of WTLW, SCLW, WTMW, and pIVS used to predict pathologic findings.

	WTLW		SCLW		WTMW		pIVS	
Variable	AUC (95% CI)	*P* value	AUC (95% CI)	*P* value	AUC (95% CI)	*P* value	AUC (95% CI)	*P* value
pN	0.711 (0.625–0.797)	<0.0001	0.796 (0.723–0.870)	<0.0001	0.809 (0.737–0.880)	<0.0001	0.788 (0.717–0.859)	<0.0001
Ly	0.685 (0.616–0.754)	<0.0001	0.793 (0.735–0.852)	<0.0001	0.801 (0.744–0.859)	<0.0001	0.772 (0.711–0.833)	<0.0001
V	0.646 (0.593–0.719)	<0.0001	0.766 (0.704–0.828)	<0.0001	0.769 (0.706–0.831)	<0.0001	0.777 (0.717–0.837)	<0.0001
pN or Ly or V	0.693 (0.623–0.762)	<0.0001	0.817 (0.761–0.873)	<0.0001	0.824 (0.769–0.879)	<0.0001	0.796 (0.733–0.855)	<0.0001
Well diff.	0.623 (0.551–0.695)	0.001	0.770 (0.710–0.830)	<0.0001	0.771 (0.711–0.832)	<0.0001	0.770 (0.709–0.830)	<0.0001

Ly, lymphatic invasion; pIVS, pathological invasion size; pN, pathological lymph node status; SCLW, solid component size of lung windows setting; V, vascular invasion; Well diff., well differentiated; WTLW, whole tumor size of lung windows setting; WTMW, whole tumor size of mediastinal setting.

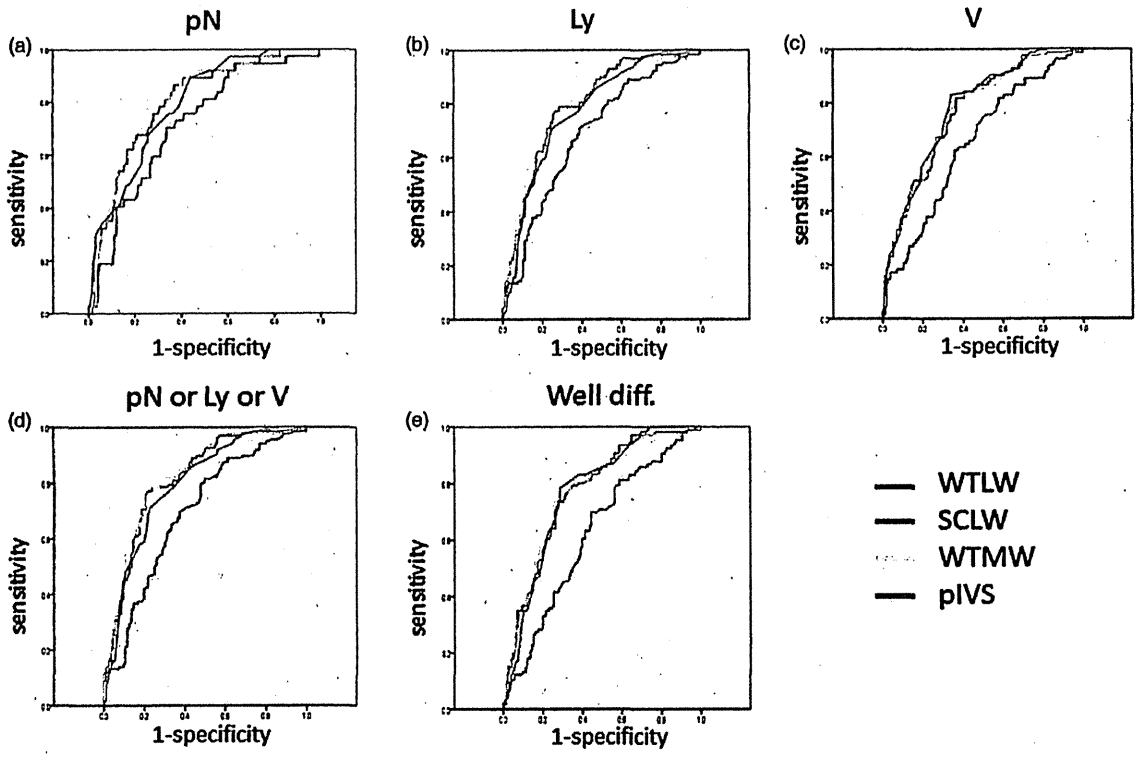

Fig. 3. Receiver operating characteristic area under the curve for detecting (a) pathological lymph node metastasis (pN), (b) lymphatic invasion (Ly), (c) vascular invasion (V), (d) high-grade malignancy (pN, VI, or PI), and (e) degree of differentiation for radiological whole and solid tumor sizes including WTLW, SCLW, and WTMW and pathological invasion area, pIVS. SCLW, solid component size of lung windows setting; WTLW, whole tumor size of lung windows setting; WTMW, whole tumor size of mediastinal setting.

whole tumor size that is WTLW for all subjects. The receiver operating characteristic curves of SCLW and WTMW were similar to that of pIVS that is pathological confirmed invasion area.

Survival significance

We assessed survival significance of preoperative radiological findings including WTLW, SCLW, and WTMW. Patients were categorized into radiological measurement of tumor size greater than 2 cm or those 2 cm or less according to WTLW, SCLW, and WTMW. There were significant differences in both the DFS and OS of this series according to SCLW ($P=0.0001$ and $P=0.023$) and WTMW ($P<0.0001$ and $P=0.008$), respectively (Fig. 4). Moreover, to find the most valuable and independent radiological prognostic factor including WTLW, SCLW, and WTMW as a candidate of next T factor, we performed multivariate analysis of DFS and OS. Table 3 revealed that WTMW (HR=0.72, 95% CI=0.58–0.90, $P=0.004$ and HR=0.74, 95% CI=0.57–0.96, $P=0.022$, respectively) was the independent prognostic factor among preoperative variables among age, sex, WTLW, and SCLW in this series.

Discussion

The frequency of identification of small lung cancers has increased since CT and enhanced scanning have become routine procedures. Small tumors, especially in lung adenocarcinomas, often contain GGO components as visualized on HRCT (2,7–9). Noguchi et al. first reported that type A and B small peripheral adenocarcinomas (localized bronchioloalveolar carcinoma without foci of active fibroblastic proliferation) showed no lymph node metastasis and a favorable prognosis (100% 5-year survival rate) (10). In 2011, new concepts were introduced including AIS and MIA. Because some of these cancers did not show growth for a long period, controversy remains as to how to manage subsolid nodules (11–14). Furthermore, both subsolid nodules and AIS have been discussed in relation to over diagnosis, which is defined as a diagnosis of lung cancer that would not lead to an individual's death because of the slow

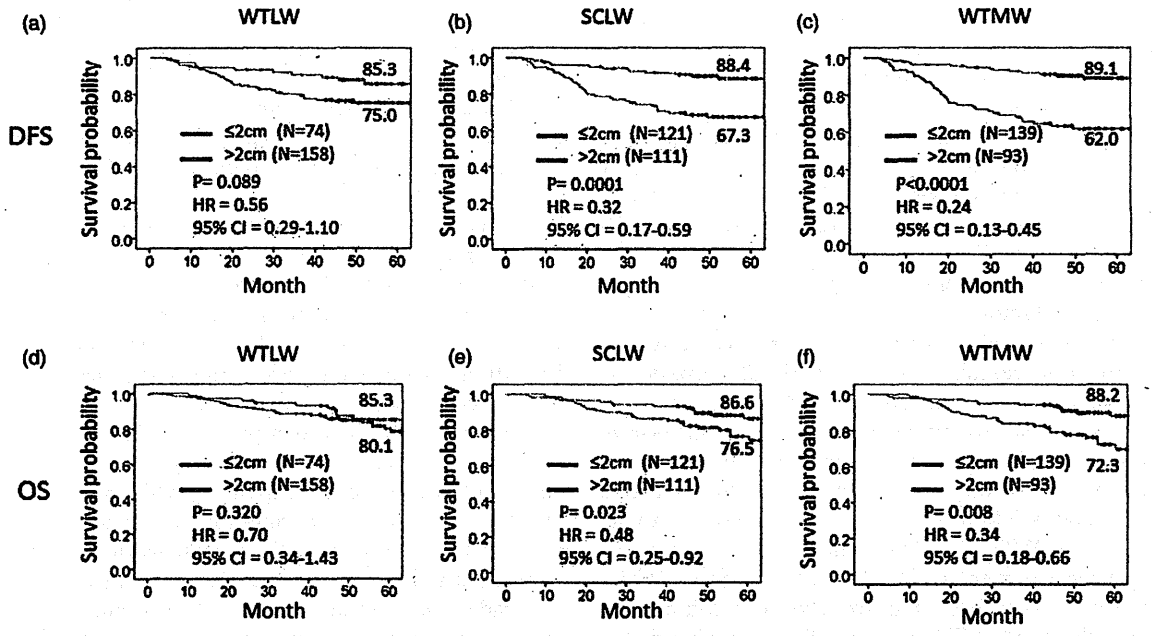

Fig. 4. Disease-free survival (DFS) and overall survival (OS) curves of patients according to tumor size on HRCT. (a) five-year DFS rate of 85.3% and 75.0% for a WTLW of 2.0 cm or less and greater than 2.0 cm, respectively ($P = 0.089$). (b) five-year DFS rate of 88.4% and 67.3% for a SCLW of 2.0 cm or less and greater than 2.0 cm, respectively ($P = 0.0001$). (c) five-year DFS rate of 89.1% and 62.0% for a WTMW of 2.0 cm or less and greater than 2.0 cm, respectively ($P < 0.0001$). (d) five-year OS rate of 85.2% and 80.1% for a WTLW of 2.0 cm or less and greater than 2.0 cm, respectively ($P = 0.320$). (e) five-year OS rate of 86.6% and 76.5% for a SCLW of 2.0 cm or less and greater than 2.0 cm, respectively ($P = 0.023$). (f) five-year OS rate of 88.2% and 72.3% for a WTLW of 2.0 cm or less and greater than 2.0 cm, respectively ($P = 0.008$). SCLW, solid component size of lung windows setting; WTLW, whole tumor size of lung windows setting; WTMW, whole tumor size of mediastinal setting.

Table 3. Multivariate analysis of DFS and OS.

		DFS			OS		
Variable	Category	HR	95% CI	*P* value	HR	95% CI	*P* value
Age (years)	<70						
	≥70	1.57	0.82–3.01	0.177	1.14	0.57–2.26	0.715
Sex	Men						
	Women	0.97	0.54–1.74	0.911	0.603	0.30–1.20	0.148
WTLW		0.94	0.89–1.00	0.040*	0.97	0.92–1.03	0.345
SCLW		0.82	0.66–1.01	0.067	0.80	0.62–1.03	0.078
WTMW		0.72	0.58–0.90	0.004 *	0.74	0.57–0.96	0.022*

*Statistically significant.

CI, confidence interval; DFS, disease-free survival; HR, hazard ratio; OS, overall survival; SCLW, solid component size of lung windows setting; WTLW, whole tumor size of lung windows setting; WTMW, whole tumor size of mediastinal setting.

growth rate and competing age-related risks for death (15–18).

The general concept of TNM classification by UICC is that "For consistency, in the TNM system, carcinoma in situ is categorized as Stage 0", according to the 7^{th} edition of the TNM Classification of Malignant Tumours (19), which means AIS itself should not be used for staging grouping. However, clinical physicians specializing in lung cancer measure the tumor size by including the GGO components visualized on HRCT. On the basis of our hypothesis that the solid components, not the GGO components, of tumors as

visualized on HRCT, indicate malignancy and prognosis, we evaluated the role of solid tumor size (the size without the GGO component) in cases of lung adenocarcinoma.

First, we demonstrated that correlations between radiological findings including WTLW, SCLW, or WTMW, and pathological findings including pWT or pIVS. There were significant correlations between pIVS and SCLW or WTMW and between pWT and WTLW. Next we analyzed sensitivity and specificity of these radiological factors for predicting pathological malignant factors including lymph node involvement, lymphatic invasion, vascular invasion, and differentiation of the tumor. All receiver operating characteristic areas under the curves for predicting pN, Ly, V, high-grade malignancy (pN or Ly or V) and well differentiation were greater in the solid components size which is SCLW and WTMW than those for the whole tumor size which is WTLW. Because the range of mean radiological measurement of WTLW, SCLW and WTMW were from 1.87 to 2.59 cm in size and the cutoff point of 2 cm is also used as T factor. Finally, we analyzed each DFS and OS according to the cutoff point of 2 cm using whole and solid tumor sizes. Kaplan-Meier curves of both DFS and OS showed better division according to the solid components size, SCLW and WTMW, compared with the whole tumor size, WTLW. Moreover, multivariate analysis revealed that WTMW were identified as independent predictive factors for both DFS and OS. These results indicate that solid tumor size, not whole tumor size, more closely reflects the pathologic findings and those related to clinical tumor malignancy.

Several investigators have reported that the prognosis of patients with lung adenocarcinoma and a large GGO component visualized on HRCT was much better than that of patients with other adenocarcinoma types, irrespective of the maximal tumor dimension (20–23). In addition, JCOG0201, a multicenter prospective radiological study has examined the specificity, sensitivity, and accuracy of the radiologic diagnoses of lymphatic/vessel invasion and nodal involvement of clinical T1N0M0 adenocarcinoma made according to the HRCT findings (24). Recently, a multicenter registration study demonstrated that solid tumor size on HRCT and maximum standardized uptake values on PET/CT has greater predictive value for high-grade malignancy and prognosis in clinical stage IA lung adenocarcinoma than that of whole tumor size (25). This final result indicated that using the solid tumor size is much simpler than using the GGO ratio; furthermore, the solid tumor size can be applied to the T descriptor in the TNM classification.

In this study, patients with lung adenocarcinoma were eligible for assessment and approximately one-third of the patients with whole tumors greater than 3 cm were included in final analysis. This confirmation of the significance of using the solid component for prognosis is consistent with previous studies using small-sized lung adenocarcinoma. Therefore, this result suggested that this concept of using solid tumor size can be applied to the T descriptor of TNM classification for larger tumors.

To the best of our knowledge, this is the first study demonstrating the correlation between radiological and pathological findings and the prognostic significance of solid tumor size in lung adenocarcinoma including tumors larger than 3 cm. However, there are several limitations in this study. First, this was a medium-size retrospective, single-institution analysis. Second, to clarify and simplify measuring the radiological and pathological size, we excluded lung adenocarcinoma with scattered invasive components which were slightly less than 10% of the population. It remains unclear whether we should count the largest scattered invasive components or the sum total of them. Third, we used two radiological measurements, SCLW and WTMW, in this analysis. Our results suggested that using WTMW counting for solid invasive components might be a better mediator for prognostic outcome of lung adenocarcinoma compared with SCLW, which is consistent with some of the previous. It remains unclear whether WTMW or SCLW should be a better predictor. Therefore, larger and multicenter studies using identical protocols are needed.

In conclusion, the predictive values of solid tumor size visualized on HRCT especially in mediastinal windows for pathologic high-grade malignancy and prognosis in patients with lung adenocarcinoma were greater than those of the whole tumor size. We recommend that the solid tumor size be used to determine the T descriptor in the TNM classification of lung tumor and be defined as the true tumor size in cases of lung adenocarcinoma with a GGO component visualized on HRCT.

Acknowledgements

We are indebted to Professor James M. Vardaman of Waseda University and Professor J Patrick Barron, Chairman of the Department of International Medical Communications of Tokyo Medical University, for their editorial review of the English manuscript.

Conflict of interest

None declared.

Funding

This study was supported by a Grant-in-Aid for Scientific Research, Japan Society for the Promotion of Science (24592104), Ministry of Education, Culture, Sports, Science and Technology, Japan.

References

1. Aberle DR, Adams AM, Berg CD, et al. Reduced lung-cancer mortality with low-dose computed tomographic screening. N Engl J Med 2011;365:395–409.
2. Nakata M, Saeki H, Takata I, et al. Focal ground-glass opacity detected by low-dose helical CT. Chest 2002;121: 1464–1467.
3. Travis WD, Brambilla E, Noguchi M, et al. International Association for the Study of Lung Cancer/American Thoracic Society/European Respiratory Society: international multidisciplinary classification of lung adenocarcinoma: executive summary Proc Am Thorac Soc 2011;8:381–385.
4. Lee HJ, Goo JM, Lee CH, et al. Predictive CT findings of malignancy in ground-glass nodules on thin-section chest CT: the effects on radiologist performance. Eur Radiol 2009;19:552–560.
5. Goldstraw P, Crowley J, Chansky K, et al. The IASLC Lung Cancer Staging Project: proposals for the revision of the TNM stage groupings in the forthcoming (seventh) edition of the TNM Classification of malignant tumours. J Thorac Oncol 2007;2:706–714.
6. Travis WD, Brambilla E, Muller-Hermelink H, et al. World Health Organization Classification of Tumours: Pathology & Genetics Tumours of the Lung, Pleura, Thymus and Heart, 3rd edn. Lyon: IARC Press, 2004.
7. Okada M, Koike T, Higashiyama M, et al. Radical sublobar resection for small-sized non-small cell lung cancer: a multicenter study. J Thorac Cardiovasc Surg 2006;132: 769–775.
8. Nakayama H, Yamada K, Saito H, et al. Sublobar resection for patients with peripheral small adenocarcinomas of the lung: surgical outcome is associated with features on computed tomographic imaging. Ann Thorac Surg 2007;84:1675–1679.
9. Suzuki K, Kusumoto M, Watanabe S, et al. Radiologic classification of small adenocarcinoma of the lung: radiologic-pathologic correlation and its prognostic impact. Ann Thorac Surg 2006;81:413–419.
10. Noguchi M, Morikawa A, Kawasaki M, et al. Small adenocarcinoma of the lung. Histologic characteristics and prognosis. Cancer 1995;75:2844–2852.
11. Kodama K, Higashiyama M, Yokouchi H, et al. Natural history of pure ground-glass opacity after long-term follow-up of more than 2 years. Ann Thorac Surg 2002; 73:386–92; discussion 92–93.
12. Takashima S, Maruyama Y, Hasegawa M, et al. CT findings and progression of small peripheral lung neoplasms having a replacement growth pattern. Am J Roentgenol 2003;180:817–826.
13. Hiramatsu M, Inagaki T, Matsui Y, et al. Pulmonary ground-glass opacity (GGO) lesions-large size and a history of lung cancer are risk factors for growth. J Thorac Oncol 2008;3:1245–1250.
14. Sawada S, Komori E, Nogami N, et al. Evaluation of lesions corresponding to ground-glass opacities that were resected after computed tomography follow-up examination. Lung Cancer 2009;65:176–179.
15. Henschke CI, Yankelevitz DF, Mirtcheva R, et al. CT screening for lung cancer: frequency and significance of part-solid and nonsolid nodules. Am J Roentgenol 2002; 178:1053–1057.
16. Toyoda Y, Nakayama T, Kusunoki Y, et al. Sensitivity and specificity of lung cancer screening using chest low-dose computed tomography. Br J Cancer 2008;98: 1602–1607.
17. Jett JR. Limitations of screening for lung cancer with low-dose spiral computed tomography. Clin Cancer Res 2005;11:4988s–4992s.
18. Goo JM, Park CM, Lee HJ. Ground-glass nodules on chest CT as imaging biomarkers in the management of lung adenocarcinoma. Am J Roentgenol 2011;196: 533–543.
19. Sobin LH, Gospodarowicz MK, Wittekind C. TNM Classification of Malignant Tumours. Oxford: John Wiley & Sons, Ltd., 2009.
20. Aoki T, Tomoda Y, Watanabe H, et al. Peripheral lung adenocarcinoma: correlation of thin-section CT findings with histologic prognostic factors and survival. Radiology 2001;220:803–809.
21. Suzuki K, Asamura H, Kusumoto M, et al. "Early" peripheral lung cancer: prognostic significance of ground glass opacity on thin-section computed tomographic scan. Ann Thorac Surg 2002;74:1635–1639.
22. Ohde Y, Nagai K, Yoshida J, et al. The proportion of consolidation to ground-glass opacity on high resolution CT is a good predictor for distinguishing the population of non-invasive peripheral adenocarcinoma. Lung Cancer 2003;42:303–310.
23. Tsutani Y, Miyata Y, Yamanaka T, et al. Solid tumors versus mixed tumors with a ground-glass opacity component in patients with clinical stage IA lung adenocarcinoma: Prognostic comparison using high-resolution computed tomography findings. J Thorac Cardiovasc Surg 2013;146:17–23.
24. Suzuki K, Koike T, Asakawa T, et al. A prospective radiological study of thin-section computed tomography to predict pathological noninvasiveness in peripheral clinical IA lung cancer (Japan Clinical Oncology Group 0201). J Thorac Oncol 2011;6:751–756.
25. Tsutani Y, Miyata Y, Nakayama H, et al. Prognostic significance of using solid versus whole tumor size on high-resolution computed tomography for predicting pathologic malignant grade of tumors in clinical stage IA lung adenocarcinoma: a multicenter study. J Thorac Cardiovasc Surg 2012;143:607–612.

Cytotherapy, 2015; 17: 330–335

International Society for Cellular Therapy
ISCT®

Safety and tolerability of allogeneic dendritic cell vaccination with induction of Wilms tumor 1–specific T cells in a pediatric donor and pediatric patient with relapsed leukemia: a case report and review of the literature

SHOJI SAITO[1,2], RYU YANAGISAWA[1,2], KENTARO YOSHIKAWA[1,2], YUMIKO HIGUCHI[1], TERUTSUGU KOYA[1], KIYOSHI YOSHIZAWA[1], MIYUKI TANAKA[2], KAZUO SAKASHITA[2], TAKASHI KOBAYASHI[1], TAKASHI KURATA[2], KOICHI HIRABAYASHI[2], YOZO NAKAZAWA[2], MASAAKI SHIOHARA[2], YOSHIKAZU YONEMITSU[3], MASATO OKAMOTO[4], HARUO SUGIYAMA[5], KENICHI KOIKE[2] & SHIGETAKA SHIMODAIRA[1]

[1]Center for Advanced Cell Therapy, Shinshu University Hospital, Matsumoto, Japan, [2]Department of Pediatrics, Shinshu University School of Medicine, Matsumoto, Japan, [3]R&D Laboratory for Innovative Biotherapeutics, Kyushu University Graduate School of Pharmaceutical Sciences, Fukuoka, Japan, [4]Department of Advanced Immunotherapeutics, Kitasato University School of Pharmacy, Tokyo, Japan, and [5]Functional Diagnostic Science, Osaka University Graduate School of Medicine, Osaka, Japan

Abstract

A 15-year-old girl with acute lymphoblastic leukemia received allogeneic dendritic cell vaccination, pulsed with Wilms tumor 1 (WT1) peptide, after her third hematopoietic stem cell transplantation (HSCT). The vaccines were generated from the third HSCT donor, who was her younger sister, age 12 years. The patient received 14 vaccines and had no graft-versus-host disease or systemic adverse effect, aside from grade 2 skin reaction at the injection site. WT1-specific immune responses were detected after vaccination by both WT1-tetramer analysis and enzyme-linked immunosorbent spot assay. This strategy may be safe, tolerable and even feasible for patients with a relapse after HSCT.

Key Words: *dendritic cells, ELISPOT, HSCT, tetramer analysis, Wilms tumor 1*

Introduction

The outcome of patients with relapsed leukemia after allogeneic hematopoietic stem cell transplantation (HSCT) is discouraging and indicates an urgent need for new therapies [1]. Donor lymphocyte infusion (DLI) has been proposed to overcome leukemic relapse after HSCT by boosting graft-versus-leukemia effect. However, DLI provokes unmanageable graft-versus-host disease (GVHD) because many allogeneic antigens are targeted by donor T cells [2].

Leukemic antigen-specific autologous dendritic cell (DC)-based vaccination for hematological malignancies is currently explored to avoid off-target effects [3,4]. The autologous DC therapy requires the production of DC vaccines from patient-derived peripheral blood mononuclear cells (PBMCs) through the use of leukapheresis. Although healthy donor-derived PBMCs may be available to generate the allogeneic DC vaccines in the patients who received HSCT, little has been reported on the safety and tolerability of the production and administration of donor-derived DCs for the donor and recipient. Additionally, the induction of leukemic antigen-specific T cells by allogeneic DC vaccines remains unclear.

Thus, we conducted a phase I clinical trial to test the safety and tolerability of Wilms tumor 1 (WT1)-specific allogeneic DC vaccination for pediatric patients with relapsed leukemia after HSCT. We report the results from the first patient who completed the allogeneic DC vaccination.

Correspondence: **Shigetaka Shimodaira**, MD, PhD, Center for Advanced Cell Therapy, Shinshu University Hospital, 3–1–1 Asahi, Matsumoto 390–8621, Japan. E-mail: shimodai@shinshu-u.ac.jp

(Received 4 June 2014; accepted 2 October 2014)

ISSN 1465-3249
http://dx.doi.org/10.1016/j.jcyt.2014.10.003

Methods

Patients

This clinical trial (UMIN: 000002105) was approved by the institutional review board of the Shinshu University School of Medicine. Written informed consent was obtained from patients over 12 years of age, HSCT donors and their parents, according to the *Helsinki Declaration*. Adverse effects were graded by use of the National Cancer Institute's Common Toxicity Criteria version 3.

Preparation of allogeneic DC vaccine

Mature DCs (mDCs) were generated under Good Manufacturing Practice conditions and cryopreserved in liquid nitrogen as described previously [5], with some modification. Briefly, a PBMC-rich fraction was obtained from the HSCT donor by means of leukapheresis with the use of the COM.TEC, cell separator (Fresenius Kabi Japan K.K., Tokyo, Japan). The PBMCs were isolated from leukapheresis products by use of Ficoll-Hypaque gradient-density centrifugation as described previously and placed into 100-mm plastic tissue-culture plates (Becton Dickinson Labware, Franklin Lakes, NJ, USA) in AIM-V medium (Gibco, Gaithersburg, MD, USA). After 30 min of incubation, nonadherent cells were removed and adherent cells were cultured in AIM-V medium. On the next day, 50 ng/mL of granulocyte-macrophage colony-stimulating factor (Gentaur, Brussels, Belgium) and 50 ng/mL of interleukin-4 (R&D Systems Inc, Minneapolis, MN, USA) were added to generate immature DCs. After 5 days of culture, immature DCs were subsequently stimulated with 10 μg/mL of OK-432 (streptococcal preparation, Chugai Pharmaceutical Co, Ltd, Tokyo, Japan) and 50 ng/mL of prostaglandin E2 (Daiichi Fine Chemical Co, Ltd, Toyama, Japan) for 24 hours to generate mDCs. The mDCs were cryopreserved and kept in liquid nitrogen until the day of administration. Cell culture supernatant is collected for sterility testing at the time of freezing. Surface molecules expressed by the DCs were determined by means of flow cytometry. The phenotype cluster of differentiation (CD) 14^-, human leukocyte antigen (HLA)-DR^+, HLA-ABC^+, $CD80^+$, $CD83^+$, $CD86^+$, $CD40^+$ and $CCR7^+$ were defined as mDCs [6].

For each vaccination, an aliquot of frozen mDCs was thawed just before clinical use and loaded with 100 μg/mL of HLA-A*24:02-restricted modified WT1 peptide (CYTWNQML, residue 235–243) and 1–2KE of OK-432 adjuvant.

Release criteria

Release criteria for administering the DC vaccine to patients include purity >90%, viability >80%, mDC phenotype, negative culture for bacteria and fungi after 14 days, endotoxin testing $\leq$ 0.05 EU/mL and negative result for mycoplasma.

Tetramer staining

Unstimulated PBMCs were stained with phycoerythrin-conjugated human immunodeficiency virus/HLA-A*24:02 tetramer as a negative control for phycoerythrin-conjugated WT1-modified peptide/HLA-A*24:02 tetramer (MBL, Medical & Biological Laboratories Co, Ltd, Nagoya, Japan), allophycocyanin-conjugated anti-human CD3 monoclonal antibodies (mAb) (Biolegend, San Diego, CA, USA) and fluorescein isothiocyanate–conjugated anti-human CD8 mAb (Beckman Coulter, Miami, FL, USA) and then were analyzed by means of flow cytometry (FACSCalibur, BD Biosciences, San Jose, CA, USA).

Enzyme-linked immunosorbent spot assay

The enzyme-linked immunosorbent spot (ELISPOT) assay was performed to examine WT1-specific interferon (INF)-γ production by $CD8^+$ T cells by use of the human interferon (IFN)-γ ELISpot PLUS kit (Mabtech, Nacka Strand, Sweden) according to the manufacturer's instructions. Briefly, the $CD8^+$ cells were isolated from the patient's PBMCs at each time point through the use of microbead-conjugated CD8 mAbs (Miltenyi Biotec, San Diego, CA, USA) and were then cultured (5×10^3 cells/well) in the presence of $WT1_{235-243}$ peptide and the $CD8^-$ cells from the PBMCs at the time of initial vaccination as stimulator cells. After 20 hours of incubation, the spots were counted by an automated ELISPOT reader (AID EliSpot Reader Classic ELR 07, Autoimmun Diagnostika GmbH, Strassberg, Germany).

Case report

Transplantations and lymphocyte infusions

A 12-year-old girl was diagnosed with B-precursor acute lymphoblastic leukemia. She underwent allogeneic bone marrow transplantation from her mother (HLA 8/8 allele-match) in first complete remission (CR) (first HSCT, Figure 1). The engraftment was successful, but she had a hematological relapse 11 months after this first HSCT. A combination of chemotherapy and two sessions of donor lymphocyte infusion (DLI) did not induce long-term remission. Consequently, she was transplanted with peripheral blood stem cells from the same donor (second HSCT, Figure 1) and successfully achieved a third CR. However, a third hematological relapse occurred

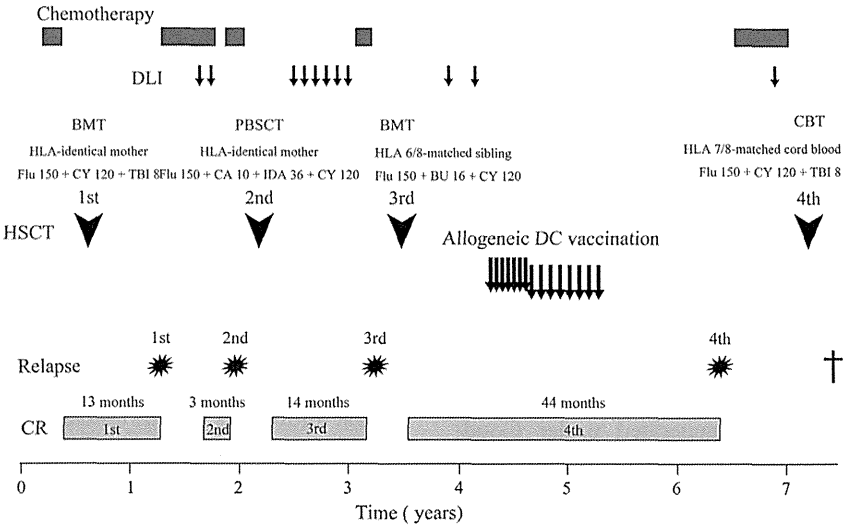

Figure 1. Clinical course of the patient. Allogeneic DC vaccination initiated 13 months after the third HSCT. BMT, bone marrow transplantation; CBT, cord blood transplantation; Flu 150, fludarabine 150 mg/m^2; CY 120, cyclophosphamide 120 mg/kg; TBI 8, total body irradiation 8 Gy; CA 10, cytarabine 10 g/m^2; IDA, idarubicin 36 mg/m^2; BU 16, busulfan (intravenously) 16 mg/kg.

14 months after the second HSCT. Therefore, she received bone marrow transplantation from her HLA 6/8–matched (A and DR alleles mismatched) sister in the third relapse (third HSCT, Figure 1). She successfully achieved neutrophil engraftment on day 16 and a fourth CR on 55. On day 50, she had grade 2 acute GVHD, but her condition was promptly improved by increasing the dose of tacrolimus. All immunosuppressants were discontinued by day 75. Additionally, she received two sessions of prophylactic DLIs (0.1 or 1 $\times$ 10^6 CD3$^+$ cells/kg) from her third HSCT donor on days 105 and 245.

Allogeneic DC vaccination

At 15 years of age, the patient was referred to our center for enrollment in a clinical study on allogeneic DC vaccination. She and her 12-year-old sister (third HSCT donor) had identical HLA-A*24:02 alleles. At the time of the third relapse, WT1 messenger RNA (mRNA) was overexpressed in the bone marrow (BM) (1.6 $\times$ 10^4 copies/μg RNA) and peripheral blood (PB) (1.5 $\times$ 10^3 copies/μg RNA), which included 1% and 42.6% blasts, respectively (Supplementary Figure 1). Therefore, they met the eligibility criteria for the clinical trial (UMIN: 000002105). Written informed consent was obtained from the patient, the third HSCT donor and their parents.

PBMCs were obtained from the donor by means of leukapheresis. Leukapheresis elicited no adverse effect, except for grade 1 nausea in the donor. Mature DCs were produced at the cell processing center of the Shinshu University Hospital under Good Manufacturing Practice conditions. Finally, 15 doses of DC vaccines (1 $\times$ 10^7 cells/dose) were generated from the single leukapheresis.

Allogeneic DC vaccination was started 13 months after the third HSCT (Figure 1). The patient maintained a fourth CR with no evidence of GVHD without receiving any immunosuppressive therapy at the time of initial vaccination. First, the patient received seven intradermal injections of DC vaccines pulsed with WT1$_{235–243}$ peptide, each dose given every 2 weeks. Because this initial immunization did not cause severe adverse effects, except for a grade 2 injection site reaction, the patient received seven additional vaccinations, given every 4 weeks. These booster vaccinations were well tolerated, aside from itching and grade 2 local erythema and vesicles at the injection sites. After the 14th vaccination, the patient maintained complete hematological remission with complete donor chimerism. Therefore, vaccination was discontinued at the request of the patient and her parents. No vaccination-related GVHD, pancytopenia or other systematic adverse effects developed during the 14 sessions of vaccination. Additionally, no immunosuppressive therapy was given during the vaccination.

WT1 mRNA expression in peripheral blood and recipient-specific chimerism in bone marrow were sequentially measured for detecting minimal residual disease during vaccination (Supplementary Figure 1). Both minimal residual disease markers disappeared before commencing the vaccination and were maintained below detectable levels during the vaccination.

Unfortunately, a fourth relapse occurred 44 months after the third HSCT, which was 14 months after the final vaccination. At the time of the fourth

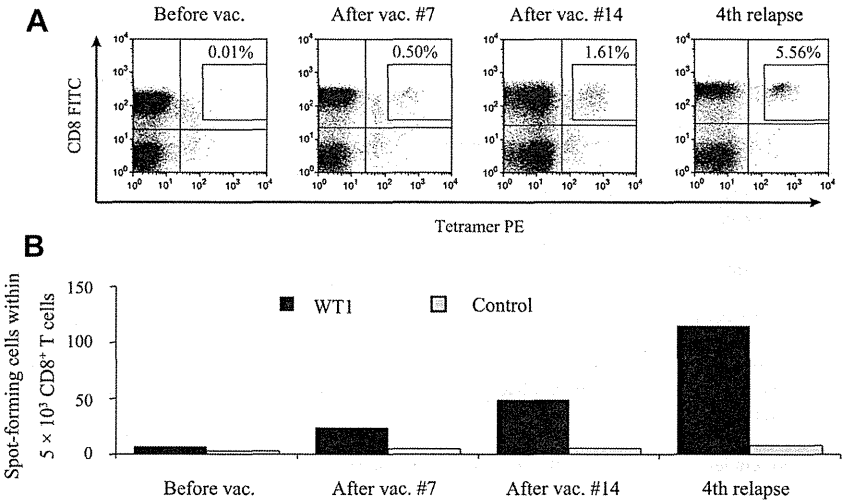

Figure 2. Impact of allogeneic DC vaccination on (vac.) (A) WT1-specific tetramer $CD8^+$ T-cell frequencies and (B) INF-γ production. (A) Tetramer staining of $CD8^+$ T cells. $WT1_{235-243}$ $tetramer^+$ $CD8^+$ T cells were detected after allogeneic DC vaccination. Shown are the frequencies of $CD8^+$ and $tetramer^+$ cells in the $CD3^+$ population. Numbers indicate the percentages of tetramer-positive cells within the $CD8^+$ population. (B) ELISPOT assays of the $CD8^+$ T cells isolated from the patient's PBMCs. WT1-specific IFN-γ secretion by $CD8^+$ T cells increased after vaccination. Histogram bars represent mean values from duplicate wells at each time point. White and black bars indicate IFN-γ secretion by $CD8^+$ T cells stimulated with human immunodeficiency virus (HIV) peptide and WT1 peptide, respectively.

relapse, WT1 mRNA was similarly overexpressed in BM (1.1×10^4 copies/μg RNA) and PB (1.3×10^3 copies/μg RNA), similar to that in the third relapse, which included 80.8% and 33.0% leukemic blasts, respectively (Supplementary Figure 1). The patient did not achieve hematological remission after chemotherapy and a single dose of DLI. Eight months after the fourth relapse, she received an HLA 7/8—matched transplant from unrelated cord blood (fourth HSCT, Figure 1). However, she died of invasive pulmonary aspergillosis 38 days after this transplant.

We closed the clinical trial only with this case because of difficulty in recruiting eligible patients.

Induction of WT1-specific immune response

$CD8^+$ $tetramer^+$ T cells were detected in the patient after the seven sessions of initial immunization, and they increased in number after the seven sessions of booster immunization (Figure 2A).

Furthermore, WT1-specific INF-γ—producing $CD8^+$ T cells were also detected after the initial immunization and were definitely increased by the booster vaccinations (Figure 2B). Interestingly, the numbers of WT1-specific INF-γ—producing $CD8^+$ T cells reached maximum values at the fourth relapse.

To determine the reasons why these functional WT1-specific T cells failed to prevent a relapse, we isolated the relapsed leukemia cells from the PBMCs by use of microbead-conjugated CD34 mAbs (Miltenyi Biotec) and performed HLA typing by use of the short-tandem repeat—polymerase chain reaction method. HLA typing was also performed on the $CD3^+$ cells isolated from the PBMCs obtained during complete remission. HLA genotyping of the $CD34^+$ leukemia cells from both third and fourth relapses showed a homozygous HLA-A*24:02/- allele, consistent with the $CD3^+$ cells.

Discussion

This study describes the treatment of the youngest donor and recipient for allogeneic DC vaccination. We successfully generated 15 doses of DC vaccine (1×10^7 cells/dose) safely from a 12-year-old, healthy donor, with a single leukapheresis session. The 14 doses of allogeneic DC vaccination pulsed with $WT1_{235-243}$ peptide were all safe and well tolerated by the 15-year-old patient, without adverse effects except for a grade 2 local reaction. A literature review identified six patients with hematological malignancies who received donor-derived allogeneic DC vaccines after HSCT, including this present case (Table I). It is noteworthy that none of them had GVHD or systemic adverse events after allogeneic DC vaccination pulsed with tumor lysate [7] or WT1 peptide [8]. Together, previous and current reports suggest that leukemia antigen—specific allogeneic DC vaccination should be safe and well-tolerated by post-transplant relapsed patients, even in pediatric patients who received allografts from their sibling donors.

WT1-specific immune responses were markedly detected after vaccination by both WT1-tetramer analysis and ELISPOT assay in our patient. WT1 antigen has been considered a promising target for

Table I. Previous case reports on allogeneic DC vaccination.

No.	Age, sex	Diagnosis	Donor characteristics (age/sex)	Pulsed with	Systemic adverse effects		Immune response		References
					GVHD	Others	Tetramer	ELISPOT	
1	24 y, F	ALL relapse	HLA-matched donor (NA/NA)	Tumor lysate	(−)	(−)	NA	NA	Fujii *et al.* [7]
2	55 y, M	AML relapse	HLA-matched donor (NA/NA)	Tumor lysate	(−)	(−)	NA	NA	Fujii *et al.* [7]
3	16 y, F	NHL relapse	HLA-matched donor (NA/NA)	Tumor lysate	(−)	(−)	NA	NA	Fujii *et al.* [7]
4	34 y, M	ALL relapse	HLA-matched donor (NA/NA)	Tumor lysate	(−)	(−)	NA	NA	Fujii *et al.* [7]
5	58 y, F	AML relapse	HLA-matched sibling (NA/NA)	$WT1_{235-243}$ peptide KLH peptide	(−)	(−)	NA	(−) (+)	Kitawaki *et al.* [8]
6[a]	12 y, F	AML relapse	HLA 7/8–matched sibling (12 y/F)	$WT1_{235-243}$ peptide	(−)	(−)	5.56%[b]	(+)	Present case

ALL, acute lymphoblastic leukemia; AML, acute myeloid leukemia; NA, not available; NHL, non-Hodgkin lymphoma; KLH, keyhole limpet hemocyanin; tetramer, tetramer assay.

[a]Present case.

[b]Shown are the maximum frequencies of the HLA-24:02–restricted WT1-tetramer$^+$ CD8$^+$ T cells within the CD8$^+$ T cells.

leukemia-specific immunotherapy. Recent clinical trials showed the feasibility and potential efficacy of WT1 peptide vaccination [9,10], or to autologous DC vaccination pulsed with WT1 peptide [3], in patients with acute myeloid leukemia or myelodysplastic syndrome. Rezvani *et al.* [11] demonstrated that the emergence of WT1-specific CD8$^+$ T cells was associated with graft-versus-leukemia effect in the patients with acute lymphoblastic leukemia after allogeneic HSCT. However, only one report was published on WT1-specific allogeneic DC vaccination [8]. A 58-year-old patient diagnosed with acute myeloid leukemia received five sessions of DC vaccines pulsed with HLA-A*24:02-restricted $WT1_{235-243}$ peptide. However, no WT1-specific immune response was detected in the patient's PBMCs by ELISPOT assay after five sessions of DC vaccination (Table I). To the best of our knowledge, we describe the first patient exhibiting a WT1-specific T-cell immune reaction after allogeneic DC vaccination.

Our patient received two sessions of DLI after the third HSCT, 5 and 10 months before the allogeneic vaccination. WT1-specific T cells have been detected in patients with multiple myeloma undergoing allogeneic HSCT and DLI [12]. Moreover, spontaneous WT1-specific T-cell responses have been reported in patients with acute myeloid leukemia [13]. Therefore, it is possible that the WT1-specific T cells were elicited by DLI or even occurred spontaneously in the patient. However, WT1-specific T cells were hardly detected at the time of initial vaccination despite two doses of DLI, whereas they were distinctly detected and increased after vaccination, which indicates that the allogeneic DC vaccination could contribute to eliciting this anti-leukemic immune response in our patient.

Interestingly, WT1-specific T-cell responses were maximal at the fourth relapse. We did not observe the loss of WT1 expression or HLA-A*24:02 allele in the relapsed leukemia cells, which could evade HLA-restricted WT1-specific T-cell response, at the time of the fourth relapse as well as the third relapse. One possible explanation for the response is that WT1-specific T cells might be merely boosted by the re-growing leukemia cells, although they were no longer able to control the disease.

Although our patient maintained less than 14 months of remission before the third HSCT, she benefited from 44 months of remission after the third HSCT with two doses of DLI and 14 DC vaccinations. These clinical observations suggest that the WT1-specific DC vaccination contributed to the longer remission after the third HSCT in our patient.

In conclusion, this report suggests that allogeneic DC vaccination is a safe, tolerable and even feasible option even for pediatric patients and pediatric donors. Because there are currently few effective therapies for patients who have a relapse after allogeneic HSCT, future trials should consider this treatment for patients with relapsing leukemia.

Acknowledgments

We wish to thank nurse Kayo Horiuchi for taking care of the patients and harvesting the PBMCs from the HSCT donor. This clinical trial was supported by Management Expense Grants from the Ministry of Education, Culture, Sports, Science and Technology, Japan (grant number: 24501330 and 24791050).

Disclosure of interests: The authors have no commercial, proprietary, or financial interest in the products or companies described in this article.

References

[1] Spyridonidis A, Labopin M, Schmid C, Volin L, Yakoub-Agha I, Stadler M, et al. Outcomes and prognostic factors of adults with acute lymphoblastic leukemia who relapse after allogeneic hematopoietic cell transplantation. An analysis on behalf of the Acute Leukemia Working Party of EBMT. Leukemia 2012;26:1211–7.

[2] Kolb HJ, Schmid C, Barrett AJ, Schendel DJ. Graft-versus-leukemia reactions in allogeneic chimeras. Blood 2004;103: 767–76.

[3] Kitawaki T, Kadowaki N, Fukunaga K, Kasai Y, Maekawa T, Ohmori K, et al. A phase I/IIa clinical trial of immunotherapy for elderly patients with acute myeloid leukaemia using dendritic cells co-pulsed with WT1 peptide and zoledronate. Br J Haematol 2011;153:796–9.

[4] Van Tendeloo VF, Van de Velde A, Van Driessche A, Cools N, Anguille S, Ladell K, et al. Induction of complete and molecular remissions in acute myeloid leukemia by Wilms' tumor 1 antigen-targeted dendritic cell vaccination. Proc Natl Acad Sci U S A 2010;107:13824–9.

[5] Kimura Y, Tsukada J, Tomoda T, Takahashi H, Imai K, Shimamura K, et al. Clinical and immunologic evaluation of dendritic cell-based immunotherapy in combination with gemcitabine and/or S-1 in patients with advanced pancreatic carcinoma. Pancreas 2012;41:195–205.

[6] Figdor CG, de Vries IJ, Lesterhuis WJ, Melief CJ. Dendritic cell immunotherapy: mapping the way. Nat Med 2004;10: 475–80.

[7] Fujii S, Shimizu K, Fujimoto K, Kiyokawa T, Tsukamoto A, Sanada I, et al. Treatment of post-transplanted, relapsed patients with hematological malignancies by infusion of HLA-matched, allogeneic-dendritic cells (DCs) pulsed with irradiated tumor cells and primed T cells. Leuk Lymphoma 2001;42:357–69.

[8] Kitawaki T, Kadowaki N, Kondo T, Ishikawa T, Ichinohe T, Teramukai S, et al. Potential of dendritic-cell immunotherapy for relapse after allogeneic hematopoietic stem cell transplantation, shown by WT1 peptide- and keyhole-limpet-hemocyanin-pulsed, donor-derived dendritic-cell vaccine for acute myeloid leukemia. Am J Hematol 2008;83:315–7.

[9] Oka Y, Tsuboi A, Taguchi T, Osaki T, Kyo T, Nakajima H, et al. Induction of WT1 (Wilms' tumor gene)-specific cytotoxic T lymphocytes by WT1 peptide vaccine and the resultant cancer regression. Proc Natl Acad Sci U S A 2004;101:13885–90.

[10] Keilholz U, Letsch A, Busse A, Asemissen AM, Bauer S, Blau IW, et al. A clinical and immunologic phase 2 trial of Wilms tumor gene product 1 (WT1) peptide vaccination in patients with AML and MDS. Blood 2009;113:6541–8.

[11] Rezvani K, Yong AS, Savani BN, Mielke S, Keyvanfar K, Gostick E, et al. Graft-versus-leukemia effects associated with detectable Wilms tumor-1 specific T lymphocytes after allogeneic stem-cell transplantation for acute lymphoblastic leukemia. Blood 2007;110:1924–32.

[12] Tyler EM, Jungbluth AA, O'Reilly RJ, Koehne G. WT1-specific T-cell responses in high-risk multiple myeloma patients undergoing allogeneic T cell-depleted hematopoietic stem cell transplantation and donor lymphocyte infusions. Blood 2013;121:308–17.

[13] Scheibenbogen C, Letsch A, Thiel E, Schmittel A, Mailaender V, Baerwolf S, et al. CD8 T-cell responses to Wilms tumor gene product WT1 and proteinase 3 in patients with acute myeloid leukemia. Blood 2002;100:2132–7.

Supplementary data

Supplementary data related to this article can be found at http://dx.doi.org/10.1016/j.jcyt.2014.10.003.

ANTICANCER RESEARCH
International Journal of Cancer Research and Treatment
ISSN: 0250-7005

Prognostic Markers for Patient Outcome Following Vaccination with Multiple MHC Class I/II-restricted WT1 Peptide-pulsed Dendritic Cells Plus Chemotherapy for Pancreatic Cancer

KAZUKI TAKAKURA[1*], SHIGEO KOIDO[1,2,3*], SHIN KAN[3], KOSAKU YOSHIDA[4], MASAKO MORI[4], YUTA HIRANO[1], ZENSHO ITO[1], HIROKO KOBAYASHI[1], SHINICHIRO TAKAMI[1], YOSHIHIRO MATSUMOTO[1], MIKIO KAJIHARA[1], TAKEYUKI MISAWA[5], MASATO OKAMOTO[6], HARUO SUGIYAMA[7], SADAMU HOMMA[3], TOSHIFUMI OHKUSA[1] and HISAO TAJIRI[1]

[1]*Division of Gastroenterology and Hepatology, Department of Internal Medicine, The Jikei University School of Medicine, Tokyo, Japan;*
[2]*Institute of Clinical Medicine and Research, The Jikei University School of Medicine, Tokyo, Japan;*
Department of [3]*Oncology and* [5]*Surgery, The Jikei University School of Medicine, Tokyo, Japan;*
[4]*Research and Development Division, Tella Inc., Tokyo, Japan;*
[6]*Department of Advanced Immunotherapeutics, Kitasato University School of Pharmacy, Tokyo, Japan;*
[7]*Department of Functional Diagnostic Science, Graduate School of Medicine, Osaka University, Osaka, Japan*

Reprinted from
ANTICANCER RESEARCH *35*: 555-562 (2015)

ANTICANCER RESEARCH

International Journal of Cancer Research and Treatment

HighWire Press STANFORD UNIVERSITY

ISSN (print): 0250-7005
ISSN (online): 1791-7530

Editorial Board

Editorial Office: International Institute of Anticancer Research, 1st km Kapandritiou-Kalamou Rd., Kapandriti, P.O. Box 22, Attiki 19014, Greece. Tel / Fax: +30-22950-53389.

E-mails: Editorial Office: journals@iiar-anticancer.org
Managing Editor: editor@iiar-anticancer.org

ANTICANCER RESEARCH supports: (a) the establishment and the activities of the INTERNATIONAL INSTITUTE OF ANTICANCER RESEARCH (IIAR; Kapandriti, Attiki, Greece); and (b) the organization of the International Conferences of Anticancer Research.

For more information about ANTICANCER RESEARCH, IIAR and the Conferences, please visit the IIAR website: www.iiar-anticancer.org

Publication Data: ANTICANCER RESEARCH (AR) is published monthly from January 2009. Each annual volume comprises 12 issues. Annual Author and Subject Indices are included in the last issue of each volume. ANTICANCER RESEARCH Vol. 24 (2004) and onwards appears online with Stanford University HighWire Press from April 2009.

Annual Subscription Rates 2015 per volume: Institutional subscription Euro 1,650.00 - print or online. Personal subscription Euro 780.00 - print or online. Prices include rapid delivery and insurance. The complete previous volumes of Anticancer Research (Vol. 1-34, 1981-2014) are available at 50% discount on the above rates.

Subscription Orders: Orders can be placed at agencies, bookstores, or directly with the Publisher. Cheques should be made payable to J.G. Delinasios, Executive Publisher of Anticancer Research, Athens, Greece, and should be sent to the Editorial Office.

Advertising: All correspondence and rate requests should be addressed to the Editorial Office.

Book Reviews: Recently published books and journals should be sent to the Editorial Office. Reviews will be published within 2-4 months.

Articles in ANTICANCER RESEARCH are regularly indexed in all bibliographic services, including Current Contents (Life Sciences), Science Citation Index, Index Medicus, Biological Abstracts, PubMed, Chemical Abstracts, Excerpta Medica, University of Sheffield Biomedical Information Service, Current Clinical Cancer, AIDS Abstracts, Elsevier Bibliographic Database, EMBASE, Compendex, GEOBASE, EMBiology, Elsevier BIOBASE, FLUIDEX, World Textiles, Scopus, Progress in Palliative Care, Cambridge Scientific Abstracts, Cancergram (International Cancer Research Data Bank), MEDLINE, Reference Update - RIS Inc., PASCAL-CNRS, Inpharma-Reactions (Datastar, BRS), CABS, Immunology Abstracts, Telegen Abstracts, Genetics Abstracts, Nutrition Research Newsletter, Dairy Science Abstracts, Current Titles in Dentistry, Inpharma Weekly, BioBase, MedBase, CAB Abstracts/Global Health Databases, Investigational Drugs Database, VINITI Abstracts Journal, Leeds Medical Information, PubsHub, Sociedad Iberoamericana de Información Científica (SIIC) Data Bases.

D.T.P. BY IIAR
PRINTED BY ENTYPO, ATHENS, GREECE
PRINTED ON ACID-FREE PAPER

ANTICANCER RESEARCH *35*: 555-562 (2015)

Prognostic Markers for Patient Outcome Following Vaccination with Multiple MHC Class I/II-restricted WT1 Peptide-pulsed Dendritic Cells Plus Chemotherapy for Pancreatic Cancer

KAZUKI TAKAKURA[1*], SHIGEO KOIDO[1,2,3*], SHIN KAN[3], KOSAKU YOSHIDA[4], MASAKO MORI[4], YUTA HIRANO[1], ZENSHO ITO[1], HIROKO KOBAYASHI[1], SHINICHIRO TAKAMI[1], YOSHIHIRO MATSUMOTO[1], MIKIO KAJIHARA[1], TAKEYUKI MISAWA[5], MASATO OKAMOTO[6], HARUO SUGIYAMA[7], SADAMU HOMMA[3], TOSHIFUMI OHKUSA[1] and HISAO TAJIRI[1]

[1]*Division of Gastroenterology and Hepatology, Department of Internal Medicine, The Jikei University School of Medicine, Tokyo, Japan;*
[2]*Institute of Clinical Medicine and Research, The Jikei University School of Medicine, Tokyo, Japan;*
Department of [3]*Oncology and* [5]*Surgery, The Jikei University School of Medicine, Tokyo, Japan;*
[4]*Research and Development Division, Tella Inc., Tokyo, Japan;*
[6]*Department of Advanced Immunotherapeutics, Kitasato University School of Pharmacy, Tokyo, Japan;*
[7]*Department of Functional Diagnostic Science, Graduate School of Medicine, Osaka University, Osaka, Japan*

Abstract. *Background/Aim: Treatment combining dendritic cells (DCs) pulsed with three types of major histocompatibility complex (MHC) class I and II (DC/WT1-I/II)-restricted Wilms' tumor 1 (WT1) peptides with chemotherapy may stabilize disease in pancreatic cancer patients. Materials and Methods: Laboratory data from seven patients with pancreatic cancer who underwent combined DC/WT1-I/II vaccination and chemotherapy were analyzed. The DC phenotypes and plasma cytokine profiles were analyzed via flow cytometry. Results: The post-treatment neutrophil to lymphocyte (N/L) ratio was a treatment-related prognostic factor for better survival. Moreover, the mean fluorescence intensities (MFIs) of human leukocyte antigen (HLA)-DR and cluster of differentiation (CD)83 on DCs were significantly increased after chemoimmunotherapy. Interestingly, interleukin (IL)-6 level in plasma was significantly increased after chemoimmunotherapy in non-super-responders. Conclusion: An increased N/L ratio, as well as HLA-DR and CD83 MFI levels may be prognostic markers of longer survival in patients with advanced pancreatic cancer who undergo chemoimmunotherapy.*

Dendritic cells (DCs) are potent antigen-presenting cells (APCs) that can present tumor-associated antigens (TAAs) in the context of class I and II (MHC-I/II) major histocompatibility complexes (MHC) and the co-stimulatory molecules cluster of differentiation (CD)80 and CD86 (1). TAAs are recognized by $CD8^+$ cytotoxic T-lymphocytes (CTLs) in the context of MHC class I (MHC-I) molecules, whereas $CD4^+$ T-cells recognize antigenic peptides in association with MHC class II (MHC-II) molecules (1). Therefore, DCs have been pulsed with various MHC-I-restricted antigenic peptides in clinical studies. However, the antitumor effects of cancer vaccine-targeting $CD8^+$ CTLs have not been investigated as vigorously in clinical trials (2).

$CD4^+$ T-cells are required for the priming, generation and maintenance of TAA-specific $CD8^+$ CTLs (1). Moreover, $CD4^+$ T-cells play a more direct role in antitumor immunity (3, 4). The Wilms' tumor 1 (WT1) antigen is highly expressed in various types of tumors, including pancreatic cancer (5), and is an excellent TAA target for cancer vaccines (6, 7). Therefore, we recently investigated the clinical and immunological responses to DCs that were pulsed with multiple MHC class I/II-restricted WT1 peptides (DC/WT1-I/II) in combination with chemotherapy for pancreatic cancer (8).

The treatment of advanced pancreatic cancer *via* DC/WT1-I/II and chemotherapy resulted in longer survival

*These Authors contributed equally to this study.

Correspondence to: Shigeo Koido, Department of Gastroenterology and Hepatology, The Jikei University School of Medicine, 163-1 Kashiwa-shita, Kashiwa, Chiba 277-8567, Japan. Tel: +81 471641111, Fax: +81 471633488, e-mail: shigeo_koido@jikei.ac.jp

Key Words: Cytokine, chemoimmunotherapy, dendritic cell, MHC class II, pancreatic cancer, vaccine, WT1.

among patients who exhibited positive delayed-type hypersensitivity (DTH) reactions against the WT1 peptides (8). Moreover, patients with strongly-positive DTH reactions maintained WT1-specific memory CTLs throughout the entire treatment period. Therefore, we suggested that a combination treatment involving DC/WT1-I/II and chemotherapy could lead to disease stability in patients with advanced pancreatic cancer (8). In the present study, we analyzed the prognostic markers for the outcomes of patients with pancreatic cancer who underwent chemoimmunotherapy with DC/WT1-I/II vaccination and chemotherapy.

Materials and Methods

Study design. The ethics committee of the Jikei Institutional Review Board at the Jikei University School of Medicine and the clinical study committee of Jikei University Kashiwa Hospital (No. 14-60 (3209) and 21-204 (6082)) reviewed and approved this study. All 7 patients with pancreatic cancer provided written informed consent and all procedures were performed in accordance with the Helsinki Declaration. All patients underwent DC/WT1-I/II vaccination and chemotherapy. The laboratory data of patients who underwent chemoimmunotherapy (*e.g.*, C-reactive protein level (CRP), lymphocyte number, neutrophil number, neutrophil to lymphocyte (N/L) ratio) were analyzed prior to and after the treatments. The N/L ratio was defined as the ratio of the number of neutrophils to the number of lymphocytes in the blood.

DC-WT1-I/II vaccines. DCs were generated from peripheral blood mononuclear cells (PBMCs) that had been prepared from leukapheresis products using Ficoll-Plaque Premium (GE Healthcare Bio-Sciences, Piscataway, NJ, USA) density gradient solution as previously described (9). The DCs were pulsed with a mixture of three WT1 peptide types that were restricted to HLA-A* 02:01, A* 02:06 (126-134: RMFPNAPYL), A*24:02 (235-243: CYTWNQMNL) and MHC-class II (332-347: KRYFKLSHLQ MHSRKH; NeoMPS Inc., City, CA, USA) (8).

Chemoimmunotherapy. The chemotherapeutic agent gemcitabine was intravenously administered at a dose of 1,000 mg/m^2 on days 1, 8 and 15 of a 28-day cycle. After the first gemcitabine administration cycle, the pancreatic cancer patients were treated with a combination of DC/WT1-I/II and gemcitabine. The DC/WT1-I/II vaccine (approximately 1×10^7 cells/dose) was intradermally administered biweekly. Nearly all vaccines overlapped with the standard chemotherapy (8).

Phenotype analysis. DCs generated from PBMCs that had been prepared from leukapheresis products were stained with the following monoclonal antibodies (mAb) for 30 min on ice: fluorescein isothiocyanate (FITC)-conjugated anti-human HLA-ABC (W6/32), CD80 (2D10), CD40 (5C3), phycoerythrin (PE)-conjugated anti-human CC chemokine receptor (CCR) 7 (150503; R&D Systems, Minneapolis, MN, USA), HLA-DR (L243), CD83 (HB 15e) and CD86 (IT2.2; BioLegend, San Diego, CA, USA). The cells were subsequently washed, fixed and analyzed using MACSQuant Analyzers (Miltenyi Biotec Inc., CA, USA) and the FlowJo analysis software (Tree Star, OR, USA).

Plasma cytokine profiles. The patient plasma samples collected were stored at −80°C. The stored plasma cytokine profiles were determined using the Human MACSPlex Cytokine 12 Kit, which enables the simultaneous measurement of human granulocyte-macrophage colony-stimulating factor (GM-CSF), interferon (IFN)-α, IFN-γ, interleukin (IL)-2, IL-4, IL-5, IL-6, IL-9, IL-10, IL-12p70, IL-17A and tumor necrosis factor (TNF)-α in a single immunoassay (Miltenyi Biotec Inc.) *via* MACSQuant Analyzers (Miltenyi Biotec Inc., CA, USA). The cytokine concentrations were quantified according to the manufacturer's instructions.

ELISA. To assess the production of IFN-γ and IL-10 in PBMCs upon stimulation with MHC-I/II-restricted WT1 peptides *in vitro*, PBMCs (1×10^6 cells/ml per well) from 6 DC/WT1-I/II vaccination cycles were cultured for 6 days with 10 μg/ml WT1 class I and II peptides in the presence of 10 U/ml recombinant human (rh) IL-2 (Shionogi, Osaka, Japan) and 10 ng/ml IL-7 (Peprotech, Rocky Hill, NJ, USA). HIV env peptides were used as negative controls. The IFN-γ and IL-10 concentrations in the sample supernatants were analyzed using ELISA kits (BioLegend) according to the manufacturer's instructions.

Statistical analysis. The statistical analyses of the overall survival (OS) and progression-free survival (PFS) prognostic factors were performed according to the Kaplan-Meier method and evaluated using the log-rank test. The immunological parameters of the pancreatic cancer patients were evaluated in a *t*-test analysis. Values were expressed as the means±standard deviation (SD). A *p*-value of <0.05 was considered statistically significant.

Results

Patients' characteristics. Patients with pathologically- or cytologically-confirmed, measurable, metastatic pancreatic adenocarcinoma or recurrent disease were enrolled in a non-comparative, open-label, phase I study (8). All 7 patients had stage IV disease and were treated with DC/WT1-I/II and chemotherapy. As shown in Table I, we identified 3 super-responders (OS>1 year) and 4 non-super-responders (OS≤1 year). After treatment, pancreatic cancer spread to the liver in one super-responder; however, this patient remains alive (>760 days) with a 100% Karnofsky Performance Status (KPS) after receiving treatment and has received more than 51 vaccinations. The remaining 2 super-responders with stage IV pancreatic cancer died at 582 and 717 days after the first treatment.

Prognostic markers as indicated by laboratory data. There were no differences between the super-responders (OS>1 year) and non-super-responders (OS≤1 year) with regard to sex, age or tumor location (Table II). We analyzed the laboratory data prior to treatment, after the first course of gemcitabine (prior to the first vaccination) and after 6-8 rounds of DC/WT1-I/II vaccination combined with gemcitabine. There was no significant difference in the lymphocyte numbers between the super-responders and non-super-responders. Moreover, the pretreatment N/L ratio of

Table I. *Patients' characteristics.*

No.	Gender	Age (years)	Location	Metastases (base line)	Previous therapy	Number of vaccines	PFS (days)	OS (days)
1	Male	70	body	Peritonitis	No	35	440	582
2	Male	68	body	Liver, Lymph nodes	Ope, Cx	46	208	717
3	Female	49	head	Liver, Peritonitis, Lymph nodes	No	7	26	133
4	Male	35	body	Liver, Lymph nodes	No	6	147	283
5	Female	72	body	Peritonitis, Lymph nodes	No	14	109	215
6	Female	69	body-tail	Lymph nodes	No	53+	545	783+
7	Male	39	head	Peritonitis	No	20	290	325

Ope: Operation, Cx: chemotherapy.

Table II. *Prognostic factors of OS or PFS.*

	OS			PFS		
	Before chemotherapy	Before vaccination	After 6-8 vaccinations	Before chemotherapy	Before vaccination	After 6-8 vaccinations
Sex (male/female)	0.427			0.427		
Age (≥65/<65)	0.207			0.464		
Ptimary tumor site (head/body-tail)	0.583			0.953		
Lymphocyte (number/μl) (≥1000/<1000)	0.953	0.197	0.863	0.646	0.694	0.207
N/L ratio (≥4/<4)	1.000	0.025*	0.018*	1.000	0.025*	0.018*
CRP (mg/dl) (≥0.5/<0.5)	1.000	0.646	0.863	1.000	0.583	0.207

OS: Overall survival, PFS: progression free survival, N/L: neutrophils/lymphocytes, CRP: C-reactive protein, *Statistically significant.

each group was not significantly associated with OS. Interestingly, after the first course of gemcitabine (prior to the first vaccination) and after 6-8 DC/WT1-I/II vaccinations combined with gemcitabine, the N/L ratio (<4) decreased significantly in the super-responders (p=0.025 and p=0.018, respectively; Table II and Figure 1). These results suggested that an N/L ratio <4 was a prognostic marker that correlated with OS.

DC phenotype. The DCs from all 7 patients displayed a characteristic phenotype comprising of HLA-ABC, HLA-DR, CD40, CD80, CD86, CD83 and CCR7 expression (Figure 2, upper panel). There were no differences in the HLA-ABC, HLA-DR, CD80, CD86, CD83 and CCR7 mean fluorescence intensities (MFIs) on DCs from super-responders (OS>1 year) *versus* non-super-responders (OS≤1 year) (Figure 3). Interestingly, the HLA-DR and CD83 MFIs were significantly increased in the DCs of the super-responders following chemoimmunotherapy (Figure 2 and Figure 4). In contrast, the CD83 MFIs in the DCs of non-super-responders decreased after therapy, although this difference was not significant (p=0.302).

Plasma cytokine level profiles. To assess the T-helper 1 (Th1) and T-helper 2 (Th2) cell-related cytokine profiles following chemoimmunotherapy, the levels of GM-CSF, IFN-α, IFN-γ, IL-2, IL-4, IL-5, IL-6, IL-9, IL-10, IL-12p70, IL-17A and TNF-α in plasma collected after 6-8 vaccinations were immediately and simultaneously analyzed. There were no differences between the super-responders and non-super-responders in terms of these plasma cytokine levels after vaccination (data not shown). The levels of immunosuppressive cytokines, such as IL-4, IL-10 and IL-6, were higher in samples from non-super-responders (OS≤1 year) than in those from super-responders (OS>1 year), although this difference was insignificant (Figure 5A). Moreover, the levels of the Th1-stimulating cytokines IFN-α, IFN-γ and TNF-α were also higher in non-responders; again, this difference was insignificant (Figure 5A). Interestingly, the IL-6 level was significantly increased after chemoimmunotherapy in non-super-responders (p=0.049) (Figure 5B).

Cytokine production by PBMCs following WT1 peptide stimulation. To assess the cytokine profiles upon WT1 peptide stimulation *in vitro* in greater detail, PBMCs were